International Journal of Biological Macromolecules xxx (xxxx) xxx–xxx

Contents lists available at ScienceDirect

International Journal of Biological Macromolecules

journal homepage: http://www.elsevier.com/locate/ijbiomac

Effect of SiO_2 nanoparticle on the physical and chemical properties of eco-friendly agar/sodium alginate nanocomposite film

Xiubin Hou [a,b,c], Zhixin Xue [a,b,c,*], Yanzhi Xia [b,c], Yimin Qin [d], Guofang Zhang [d], Hongwu Liu [d], Kechang Li [d]

[a] College of Chemistry and Chemical Engineering, Qingdao University, Qingdao 266071, China
[b] Institute of Marine Fiber Biobased Material, Qingdao University, Qingdao 266071, China
[c] State Key Laboratory of Biopolysaccharide Fibers and Ecological Textiles, Qingdao University, Qingdao 266071, China
[d] State Key Laboratory of Bioactive Seaweed Substances, Qingdao Bright Moon Seaweed Group Co., Ltd, Qingdao 266400, China

ARTICLE INFO

Article history:
Received 8 June 2018
Received in revised form 16 September 2018
Accepted 18 September 2018
Available online xxxx

Keywords:
Physiochemical properties
Food packaging
Nanocomposite film

ABSTRACT

Agar/sodium alginate (AG/SA) nanocomposite films were prepared using solution casting method in presence of various concentrations of nano-SiO_2 (2.5, 5, 7.5, and 10 wt%). The effect of nano-SiO_2 concentration on the nanocomposite film was investigated. The result of Fourier transform infrared (FTIR) illustrated the formation of hydrogen bonding between nano-SiO_2 and polysaccharide. As nano-SiO_2 concentration rose from 0 to 10 wt%, the tensile strength and elongation at break all increased up to maximum, respectively. The tensile strength and elongation at break of film containing 10 wt% nano-SiO_2 increased by 65.29% and 60.38% respectively when compared to those of film prepared without nano-SiO_2. The reason for enhancing in tensile strength might be related to the formation of molecular interaction. The film containing 2.5 wt% nano-SiO_2 had maximum water contact angle and minimum water vapor permeability among those of all films prepared in this work. However, the film containing 10 wt% nano-SiO_2 had minimum swelling degree and water solubility, further demonstrating the formation of strong interaction. The addition of nano-SiO_2 improved the properties of film against UV light and thermal stability. Overall, the addition of nano-SiO_2 enhanced the mechanical properties, water resistance and thermal stability of polysaccharide film.

1. Introduction

Because of increasing environmental concerns, great efforts have been done to extend shelf-life and quality of food while reducing post consumption packaging material, leading to development of new biopackaging materials called edible and biodegradable films made of biopolymers [1,2]. Biopolymer-based biodegradable films have been gaining attention as an alternative for nondegradable films due to their nontoxicity, biocompatibility, reproducibility, versatility and abundant availability. Edible and biodegradable film can reduce environmental problems caused by traditional packaging materials. Biodegradable materials usually are made with polysaccharides, proteins, and lipids or their combination. Among these materials, polysaccharides extracted from natural seaweed are mostly widely utilized and studied for food packaging applications due to good film forming property and mechanical and gas barrier properties compared with other biopolymeric material [3]. AG, carrageenan and SA as common nature polysaccharide have been studied to prepare biodegradable films [4–6]. But these polysaccharide films do not meet standard requirements for commercial application.

Brittleness, high water sensitivity, low thermal stability and low gas barrier properties restrict the use of pure biopolymer film in food packaging material. Thus, the films prepared through blending polysaccharide with diverse properties can obtain various characteristics of the blended raw materials, which improves the overall characteristics of composite films [5,7–9]. The blending natural polysaccharides must have high compatibility, and hydrogen bonding dipole-dipole forces or charge transfer complexes can be formed between molecules. As a fibrous carbohydrate extracted from a number of marine algae of the class Rhodophyceae, called 'red seaweeds', AG is composed of β-D-galactopyranosyl linked (1 → 4) to a 3,6-anhydro-α-L-galactopyranosyl unit with partially sulfated, and it produces perceptible gels at concentrations as low as 0.04% (Fig. 1) [10,11]. There were a tiny bit of sulfate groups on the molecular chain of AG. Being isolated from brown algae (*Laminaria digitate* and *Ascophyllum nodosum*) cell walls, alginate is a water-soluble linear anionic polysaccharide, consisting of monomeric units of 1–4-linked β-D-mannuronate (M) and α-L-guluronate (G) (Fig. 1) [12]. The water resistance of SA is poor because it is easy to dissolve in water at room temperature. AG and SA all have lots of hydroxyl groups, and SA contains some of the carboxylic acid groups. This provides the opportunity for the formation of

* Corresponding author at: College of Chemistry and Chemical Engineering, Qingdao University, Qingdao 266071, China.
E-mail address: xuezhixin@qdu.edu.cn (Z. Xue).

https://doi.org/10.1016/j.ijbiomac.2018.09.109
0141-8130/

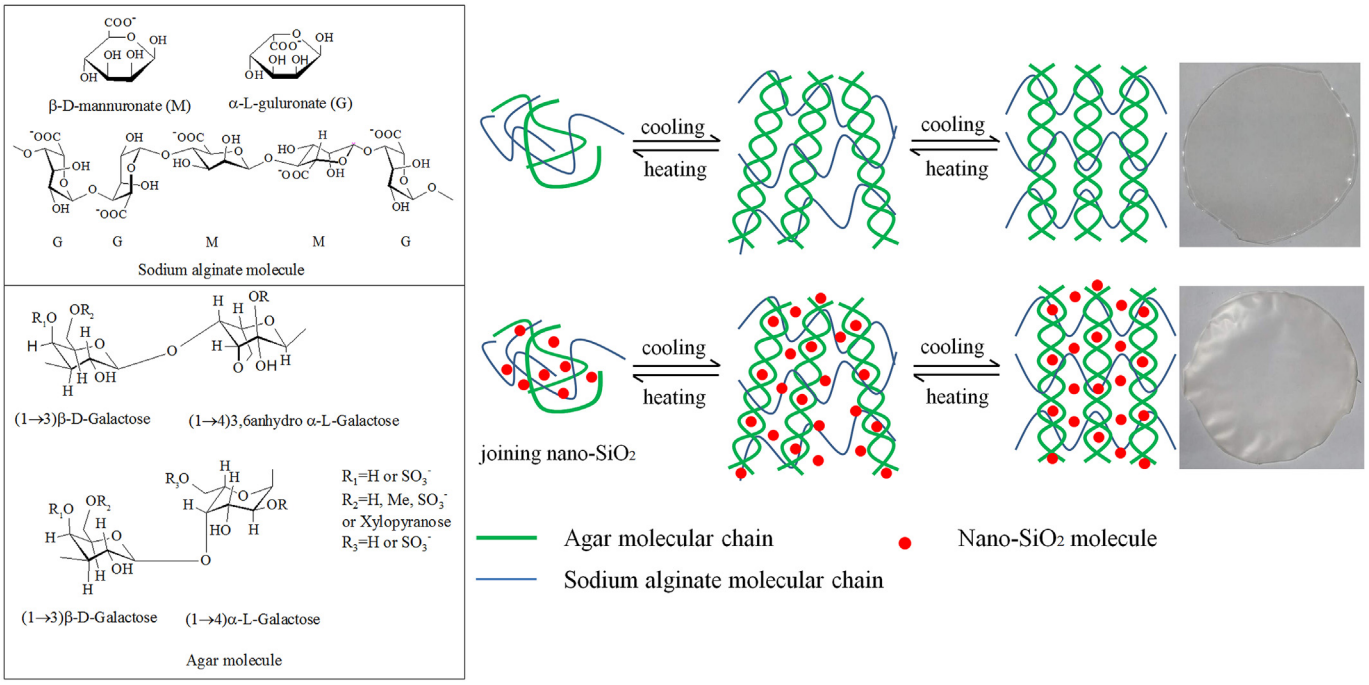

Fig. 1. Molecular structure of AG and SA and their ideal gelation mechanism diagram.

intermolecular hydrogen bonding. Their ideal gelation mechanism was shown in Fig. 1. But the properties of AG/SA composite films still cannot cater to the needs of commercialization.

Although blending biopolymer films are extremely promising food packaging material, there are some limitations to the commercial use of them due to their poor mechanical properties and high water sensitivity and low barrier properties to moisture [13]. To overcome these defect, great effort have been done through adding nanoparticles into the biopolymer films [4,14–16]. Nano-SiO_2 as cheap and nontoxic fillers has been widely added to the biopolymer materials [17–20]. As amorphous powder with tridimensional structure, nano-SiO_2 has prominent features of small size, large specific surface area, high surface energy, unsaturated chemical bonds, and hydroxyl group on the surface, which is conducive to dispersion of nano-SiO_2 in the film [21].

Many papers have reported the AG nanocomposite films, alginate nanocomposite, and biopolymer/SiO_2 nanocomposite film. However, as far as we know, there is no report to research the influence of nano-SiO_2 concentration on the physicochemical properties of AG/SA film. In this work, AG/SA nanocomposite films incorporating different nano-SiO_2 concentration were prepared. The AG/SA films without and with nano-SiO_2 were characterized by scanning electron microscopy (SEM), X-ray diffraction (XRD), and FTIR. The mechanical properties, water resistance, optical properties, surface color and thermal stability of films were examined, expecting new biodegradable films with good mechanical properties, water resistance and thermal stability.

2. Experimental

2.1. Materials

AG (Gel strength ≥ 1200 g/cm^2 at 1.5%) was purchased from Lanji technology development co., Ltd. (Shanghai, China) and was used without further purification. SA (M/G = 2:1, Mw 2.1×10^6 g/mol) was purchased from Jiejing Seaweed co., Ltd. (Rizhao, China). SiO_2 nanoparticles were purchased from Aladdin Digital Technology Co., Ltd. (Shenyang, China), ranging from 25 to 35 nm. Glycerol was purchased from Sinopharm Chemical Reagent Co., Ltd. (Shanghai, China). All the aqueous solutions were prepared using distilled water which was made in laboratory.

2.2. Preparation of films

AG/SA composite films and AG/SA/SiO_2 nanocomposite films were prepared by solution casting method [22]. Film solutions were prepared by dissolving 1 g AG powders and 1 g SA powder into 100 mL distilled water with 0.6 g glycerol as the plasticizer with mixing vigorously under 600 rpm at 95 °C for 30 min. For the preparation of the nanocomposite film solution, various amounts of SiO_2 nanopowders at the concentration of 2.5, 5, 7.5 and 10 wt% (based on the total weight of AG and SA) were dispersed respectively into 100 mL distilled water stirred vigorously at room temperature for 30 min followed by sonication for 1 h using a high-power CNC ultrasonic cleaner. The SiO_2 solutions were heated to 95 °C and subsequently 2 g total dry matter (1 g AG powder and 1 g SA powder) were added into the solution with 0.6 g glycerol with mixing vigorously under 600 rpm at 95 °C for 30 min. Next, the homogeneous solutions were statically immovable at 95 °C for 15 min to eliminate bubbles. Then the hot solutions weighing 20 ± 0.2 g were poured into the petri dishes with a diameter of 10 cm. These petri dishes were dried in the oven at 50 °C for 32 h. Finally, all resulting films were peeled off from petri dishes and then were stored in the room with a constant temperature (20 °C) and constant relative humidity (60%) for at least 48 h.

2.3. Characterization

The surface morphologies of AG/SA composite films and AG/SA/SiO_2 nanocomposite films were measured by field emission SEM (Hitachi TM-3000, Japan) at 15 kV after gold coating. The crystal morphologies of five kinds of films and SiO_2 nanoparticles were examined through XRD analysis. All film samples and SiO_2 nanopowders were put into glass supports respectively. XRD (DX2700, China) measurement were operated with Cu Xα radiation (l = 1.5418 Å) with a scan rate (2θ) of 1°/min in an angular range of 10–70 at an accelerating voltage of 40 kV and an applied current of 30 mA. The functional groups were confirmed by FTIR spectra (Thermo Fisher Scientific Nicolet iS 50, China) using 32 scans in the range of 4000–400 cm^{-1} with a resolution of 4 cm^{-1}. Zeta potential of nano-SiO_2 solution and mixed solution of AG and SA with 0.5 wt% concentration was examined using nano-laser

Please cite this article as: X. Hou, et al., Effect of SiO2 nanoparticle on the physical and chemical properties of eco-friendly agar/sodium alginate nanocomposite film, (2018), https://doi.org/10.1016/j.ijbiomac.2018.09.109

particle detector (Zetasizer Nano ZSE, England). The thermal properties of films were determined at the constant heating rate of 10 °C/min from 35 °C to 600 °C in nitrogen atmospheres using the thermogravimetric (TG) analyzer (TG209F3, Germany).

2.4. Film thickness

The thickness of all films was measured using a digital micrometer (Dial thickness gauge 7301, Mitutoyo Co., Japan). All film samples were measured ten times at different regions to obtain average values which were used to determine mechanical properties, water vapor permeability, light transmittance and opacity.

2.5. Mechanical properties

The tensile strength (TS) and elongation at break (EB) were evaluated at constant temperature (20 °C) and relative humidity (60%) using WDW-5 microcomputer control electronic universal testing machine (Jide Mechanical Engineering, Jinan, China) according to ASTM D 882 [23]. All film samples (100 mm × 20 mm) were settled between tensile grips of instrument. The initial grip separation was set to 50 mm, and crosshead speed 50 mm/min.

2.6. Moisture content

Before measuring moisture content (MC), all film samples (30 mm × 30 mm) were stored in the room with a constant temperature (20 °C) and constant relative humidity (60%) for at least 48 h, and then weighted. Next, all samples were dried in the oven at 108 °C for 8 h and weighed to determined their dry matters. The MC was calculated as following formula:

$$\mathrm{MC}\ (\%) = \frac{W_1 - W_2}{W_1} \times 100$$

where W_1 and W_2 are the weight of the film sample before and after drying.

2.7. Water contact angle

The water contact angle (WCA) of film surface was examined using a WCA analyzer (Theta Lite, Biolin Scientific Sweden). The film sample (30 mm × 70 mm) was glued on the glass plate to yield flat film. Then the glass plate was placed on the movable stage of WCA analyzer. A water drop of about 7 μL was dropped on the film surface. The WCA on both sides of the water droplet was evaluated.

2.8. Water vapor permeability

Water vapor permeability (WVP) of films was examined gravimetrically according to the ASTM E96 desiccant method described by Alboofetileh et al. [24]. The films (30 mm × 30 mm) were tightly sealed on the top of glass permeation cups (internal diameter = 25 mm) containing distilled water (100%RH, 2.337×10^3 Pa vapor pressure at 20 °C). Then the glass permeation cups with films were placed in a desiccator (1.5%RH, 28.044 Pa water vapor pressure) with silica gel at 20 °C. The weight changes of the cups were recorded at intervals of 1 h for 8 h. The water vapor transmission rate (WVTR) was calculated using the slopes of the steady-state (linear) portion of weight loss versus time curves. The WVP of film was calculated using the following formula:

$$\mathrm{WVP} = \frac{\mathrm{WVTR}}{\Delta P} \times L$$

where WVTR is the measured slope of water vapor transmission rate ($g \cdot m^{-2} \cdot s^{-2}$), L is the mean film thickness (m), and ΔP is the partial water vapor pressure difference (Pa) between the two sides of the film.

2.9. Swelling properties

The swelling properties of films were examined according to the method reported by Xu et al. [25]. The swelling degree (SD) was calculated as following formula:

$$\mathrm{SD}\ (\%) = \frac{W_2 - W_1}{W_1} \times 100$$

where W_1 and W_2 are the weight of the film sample before and after soaking in water.

2.10. Water solubility

The water solubility (WS) of films was measured using the method reported by Tunc et al. [26]. The WS was calculated using the following formula:

$$\mathrm{WS}\ (\%) = \frac{W_1 - W_2}{W_1} \times 100$$

where W_1 and W_2 are the weight of the dry matter before and after solution, respectively.

2.11. Light transmission and transparency

The light transmission and transparency of the films were determined using T9S UV–visible spectrophotometer (PERSEE, China). The film sample was fixed on the whiteboard of solid integrating sphere of the spectrophotometer. The other whiteboard was used as reference, and sample was scanned at wavelengths between 200 nm and 800 nm. The opacity value of films was calculated as following:

$$\mathrm{Opacity} = \frac{\mathrm{Abs600}}{x}$$

where Abs600 is the value of absorbance at 600 nm, and x is the film thickness (mm).

2.12. Apparent surface color

Apparent surface color of films was examined using a SC-80C automatic colorimeter (KANGTONG, China). The film sample was placed on a standard white plate ($L^* = 92.02$, $a^* = 7.51$, $b^* = 5.01$, where L^* is luminosity, a^* is red/green, and b^* corresponds to yellow/blue). The total color difference (ΔE) and whiteness index (WI) were calculated on the basis of standard plate parameters:

$$\Delta E = \sqrt{(\Delta L)^2 + (\Delta a)^2 + (\Delta b)^2}$$

$$\mathrm{WI} = 100 - \sqrt{(100 - L^*)^2 + (a^*)^2 + (b^*)^2}$$

where ΔL, Δa, and Δb are the difference between the difference between each color value of standard color plate and film specimen, respectively.

2.13. Statistical analysis

One way analysis of variance (ANOVA) was performed, and the significant difference between factors and levels was examined with Duncan's multiple range tests using an SPSS 22 statistical analysis computer program for Windows (SPSS Inc., Chicago, IL, USA). A value of $p < 0.05$ was considered significant. All measurements were repeated at least 4 times. All data were presented as means ± standard deviations.

Please cite this article as: X. Hou, et al., Effect of SiO2 nanoparticle on the physical and chemical properties of eco-friendly agar/sodium alginate nanocomposite film, (2018), https://doi.org/10.1016/j.ijbiomac.2018.09.109

3. Results and discussion

3.1. Surface morphology

The uniformity, distribution quality, agglomeration, and presence of voids of AG/SA composite film and AG/SA/SiO_2 nanocomposite film were examined by SEM in the more extensive morphological investigation, and the result was shown in Fig. 2. The surface of five kinds of films had no void and crack. The surface of films without nano-SiO_2 was smooth and homogenous. However, the surface of films with nano-SiO_2 was coarse. SiO_2 nanoparticles were dispersed homogenously in the film surface, indicating that strong interaction might be formed between nano-SiO_2 and molecules of matrix. As the concentration of nano-SiO_2 rose, the roughness of nanocomposite film surface became large, especially at 10 wt% concentration, and few small particles were presented on the surface and no obvious exfoliation was exhibited. The nano-SiO_2 concentration had slight influence on the aggregated particle size. This might be related to the energy of nano-SiO_2 associating with polysaccharide chains lower than that of self-aggregating of nano-SiO_2 in solution. The result demonstrated that strong interfacial adherence existed between nano-SiO_2 and biopolymer matrix, consistent with result reported by Yang et al. [27]. This might contribute to reinforcement of the mechanical properties and water resistance of nanocomposite films.

3.2. X-ray diffraction (XRD) and Fourier transform infrared spectroscopy (FTIR)

Molecular aggregation structure of biopolymer materials was verified through XRD analysis. Fig. 3 showed XRD pattern of AG/SA composite film and AG/SA/SiO_2 nanocomposite film. XRD spectra of nano-SiO_2 showed a broad and strong diffraction peak at 2θ of 22.64°, indicating

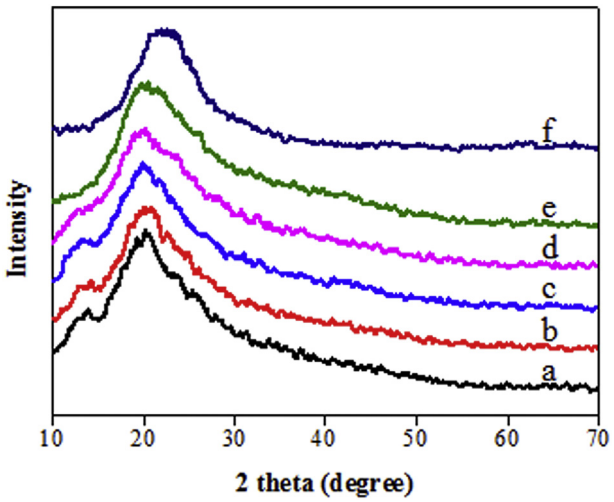

Fig. 3. XRD pattern of films (a: AG/SA; b: AG/SA - 2.5 wt% SiO_2; c: AG/SA - 5 wt% SiO_2; d: AG/SA - 7.5 wt% SiO_2; e_1: AG/SA - 10 wt%) and nano-SiO_2 (f).

the amorphous structure of nano-SiO_2. There is a weak characteristic diffraction peak at 2θ of 14.01° in the XRD spectra of AG/SA composite film. And the amorphous structure of AG/SA composite film was also confirmed by a broad and strong diffraction peak at 2θ of 20.23°. However, with the increase of nano-SiO_2 concentration in the nanocomposite film, the intensity of diffraction peak at 2θ of 14.01° gradually weakened, indicating that the crystallinity of matrix was reduced by the addition of SiO_2 [27]. For the films containing 7.5 wt% and 10 wt% nano-SiO_2, the diffraction peak at 2θ of 14.01° disappeared in the XRD, indicating formation of an exfoliated structure which was disordered

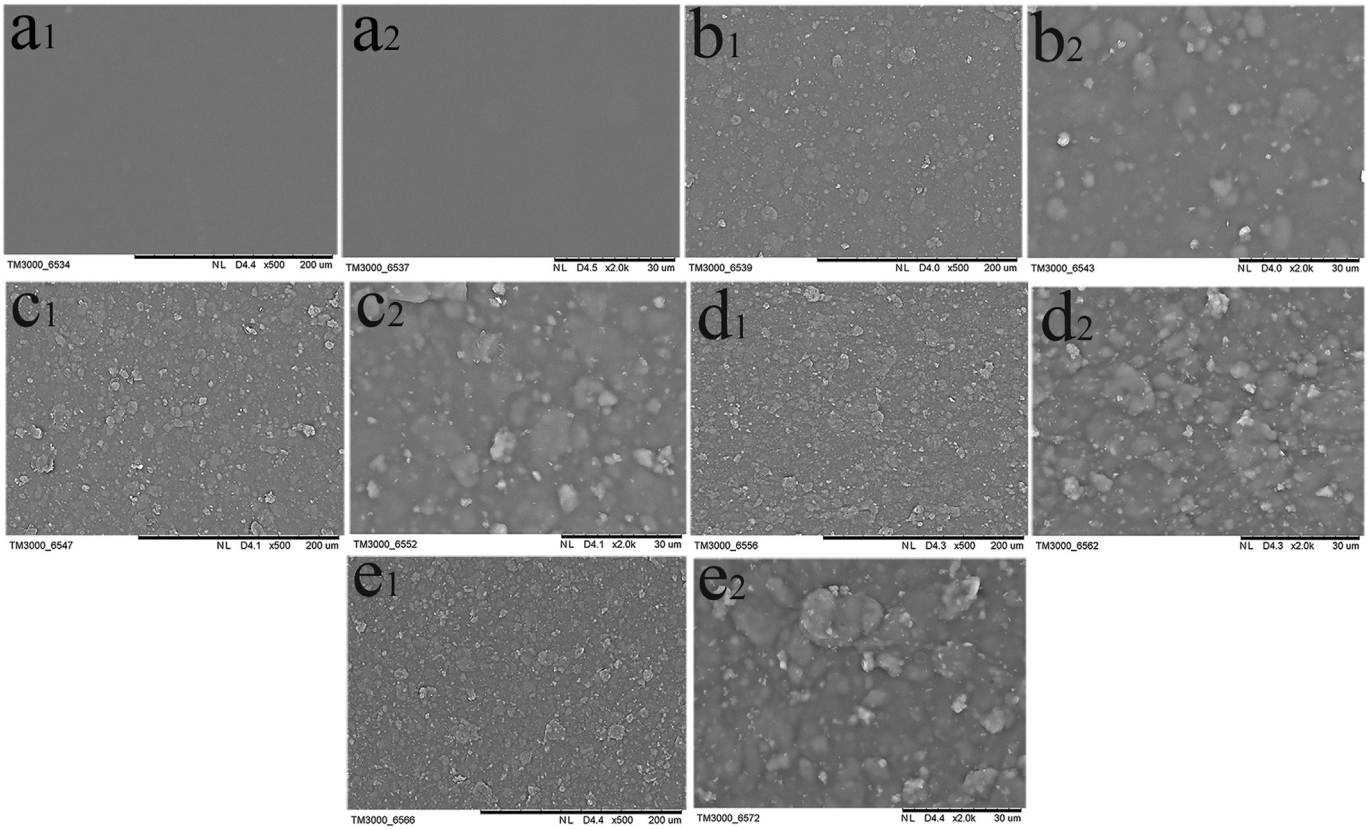

Fig. 2. SEM micrographs of the film surface (a_1, a_2: AG/SA; b_1, b_2: AG/SA - 2.5 wt% SiO_2; c_1, c_2: AG/SA - 5 wt% SiO_2; d_1, d_2: AG/SA - 7.5 wt% SiO_2; e_1, e_2: AG/SA - 10 wt%).

Please cite this article as: X. Hou, et al., Effect of SiO2 nanoparticle on the physical and chemical properties of eco-friendly agar/sodium alginate nanocomposite film, (2018), https://doi.org/10.1016/j.ijbiomac.2018.09.109

and not detectable by XRD, consistent with the result reported by Alboofetileh et al. [24]. The diffraction peak at 2θ of 20.23° gradually widened. A new diffraction peak at 2θ of 22.64° appeared in the film containing nano-SiO_2, and the diffraction peak enhanced gradually as the concentration of nano-SiO_2 rose. This phenomenon might be ascribed to the interaction formed between nano-SiO_2 and the molecule of biopolymer matrix [28,29]. The analogical consequence was shown in FTIR spectra of films.

Some functional groups of AG/SA composite film, AG/SA/SiO_2 nanocomposite film and nano-SiO_2 were preliminarily confirmed with the FTIR spectroscopy data, and the result was presented in Fig. 4. Nano-SiO_2 exhibited characteristic peaks at 1082 cm^{-1} (asymmetric stretching vibration of Si—O—Si), 798 cm^{-1} (symmetric stretching vibration of Si-O-Si) and 456 cm^{-1} (bending vibration of Si-O-Si) [30,31]. The absorption peaks at 965 cm^{-1} was due to Si—O of Si-OH [32]. The AG/SA film presented characteristic absorption peaks at 3290 cm^{-1} and 2938 cm^{-1}, which was ascribed to the stretching vibration of O—H band and symmetric and asymmetric stretching vibration of C—H band in hexatomic ring, respectively [33]. The characteristic peaks at 1600 cm^{-1} and 1406 cm^{-1} could correspond to the asymmetrical and symmetrical vibration of carbonyl group from —COO^- of SA and deformation vibration of C—H, respectively [34]. The weak peak at 1062 cm^{-1} and more intense peak at 1030 cm^{-1} were attributed to C—O and C—C stretching vibrations and to C-C-O and C-O-H deformation of pyranose ring common to all polysaccharides [34,35]. However, the absorption peak of O—H stretching vibration of AG/SA/SiO_2 film shifted to 3301 cm^{-1}. The slight change might be attributed to formation of hydrogen bonding between SiO_2 and polysaccharide. This phenomenon was similar to that reported by Tang et al. [30] and Yang et al. [28]. As nano-SiO_2 concentration rose, the peak intensity at 1062 cm^{-1} enhanced gradually. This phenomenon might be related to the molecular interaction formed between nano-SiO_2 and matrix. And the peak at 965 cm^{-1} and 456 cm^{-1} appeared in the FTIR spectrum of AG/SA/SiO_2 film, but not in that of AG/SA film. This demonstrated that nano-SiO_2 appeared in the nanocomposite film, which agreed with the result of SEM.

3.3. Zeta potential

The positive and negative charge of the solution is characterized by the zeta potential. The zeta potential of nano-SiO_2 solution and mixed solution of AG and SA was shown in Fig. 5. The zeta potential of nano-SiO_2 solution and mixed solution was −29.4 mV and −54.7 mV respectively, indicating that the aqueous solution of nano-SiO_2 and mixed solution were all negatively charged. Had been confirmed in FTIR, there were hydroxyl groups on the surface of nano-SiO_2 which contributed to the formation of hydrogen bonding between hydroxyl group of nano-SiO_2 and hydroxyl group/carboxylic group of matrix.

3.4. Thickness and mechanical properties

Table 1 showed the thicknesses of five kinds of films. The thickness of each kind of film was homogenous, further demonstrated that nano-SiO_2 dispersed homogenously in the molecular skeleton of matrix. The thickness of AG/SA film was 50.2 ± 1.17 μm, which was the highest among those of films. The reason behind this might be related to strong interaction formed between nano-SiO_2 dispersed in the matrix and molecules of matrix. The formation of hydrogen bonding made the intermolecular force of polysaccharide molecules stronger, leading to the reduction in the intermolecular spacing. Although as nano-SiO_2 concentration rose from 2.5 to 10 wt%, the thickness of nanocomposite film increased gradually. However there was no significant difference between them ($p > 0.05$). Similarly to the result of SEM, the thickness of nanocomposite film was slightly affected by the concentration of nano-SiO_2, consistent with the result reported by Yang et al. [27].

Mechanical properties of polymeric films, used as indicators for the film to maintain integrity of film and to withstand environmental stress during packaging application, are usually measured by means of TS and EB [36]. The mechanical properties have to do with the density and distribute of intra- and intermolecular interaction in the matrix. The TS and EB of all films were presented in Table 1. As the concentration of nano-SiO_2 rose, the TS of films improved gradually and reached a maximum value of 74.68 ± 2.23 MPa, higher than those of AG/alginate/collagen ternary film [37] and AG/gelation/TiO_2 nanocomposite film [38]. The TS value of film without nano-SiO_2 was 45.18 ± 1.34 MPa, significantly lower than those of films containing different concentration nano-SiO_2 ($p < 0.05$). This phenomenon indicated that the addition of nano-SiO_2 significantly enhanced the TS of polysaccharide film, which might be ascribed to reinforcement effect of homogeneously dispersed high-strength nano-SiO_2 in the matrix. The increase in TS is of vital criteria for food packaging applications as high TS can allow the packaging films to withstand the normal stress encountered during food handling, shipping, and transportation [39]. As the concentration of nano-SiO_2 rose from 2.5 to 10 wt%, the TS values of them increased by the similar interval value. The mechanical properties of film were enhanced by the interfacial interaction between nano-SiO_2 and biopolymer matrix, which might be attributed to the good dispersion of SiO_2 nanoparticles after ultrasonication in the AG and SA matrix [27]. This phenomenon might be related to strong interactions between nano-SiO_2 and the matrix via hydrogen bonding, resulting in considerable interfacial contacts between them and effective stress transfer [40]. Nano-SiO_2 with tremendous surface area had many opportunities for contact with hydroxyl groups and carboxylic groups belonging to polysaccharide molecule, which facilitated the transfer of stress from matrix to the reinforcing phase via interface [39]. At low nano-SiO_2 concentration, there were a bit of molecular interactions formed between nano-SiO_2 and the matrix. However, lots of molecular interactions were formed at high nano-SiO_2 concentration, which contributed to the further improvement of TS of film.

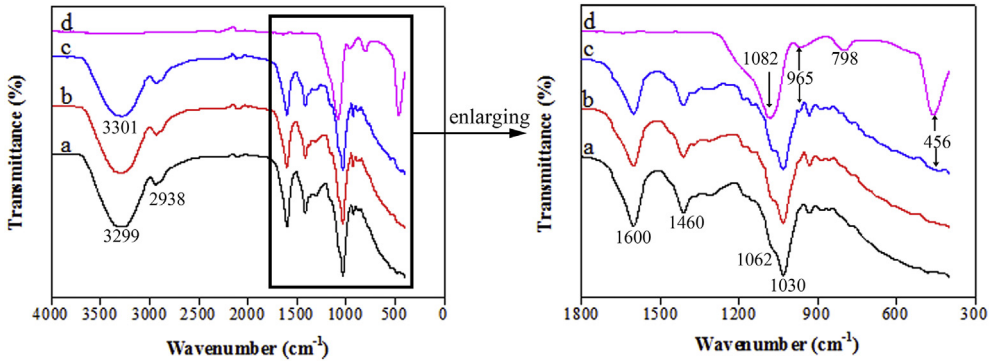

Fig. 4. FTIR spectra of film (a: AG/SA; b: AG/SA - 5 wt% SiO_2; c: AG/SA - 10 wt%) and nano-SiO_2 (d).

Please cite this article as: X. Hou, et al., Effect of SiO2 nanoparticle on the physical and chemical properties of eco-friendly agar/sodium alginate nanocomposite film, (2018), https://doi.org/10.1016/j.ijbiomac.2018.09.109

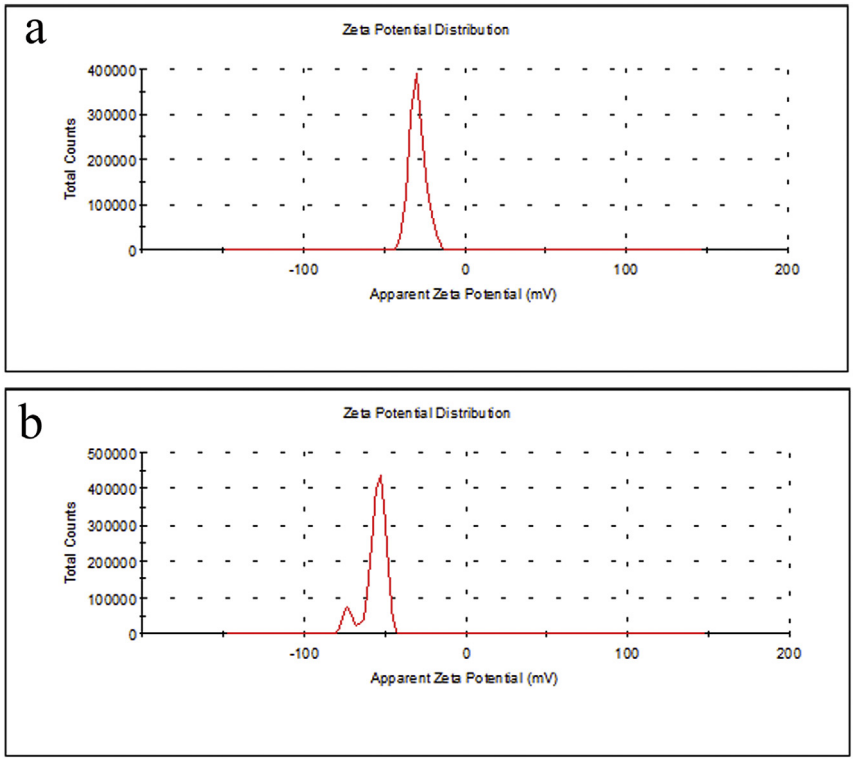

Fig. 5. Zeta potential pattern of nano-SiO_2 solution (a) and mixed solution (b).

With increase of concentration of nano-SiO_2, the EB value of five kinds of films rose gradually. This phenomenon indicated that the addition of nano-SiO_2 enhanced the elongation at break of film. The result was in good agreement with that reported by Yang et al. [27] and Tabatabaei et al. [40]. The EB of film incorporating 10 wt% nano-SiO_2 was significantly higher than those of other four films ($p < 0.05$). As shown in SEM, SiO_2, playing the role of plasticization, dispersed homogeneously with few agglomerations in the nanocomposite film. The effect of plasticization enhanced gradually with increase of nano-SiO_2 concentration. Nanoscale SiO_2 particles homogeneously dispersed in the molecular skeleton of matrix, which might influence intra- or interaction of polysaccharide chain. This was conducive to the mutual rearrangements of chain unit, thereby improving flexibility of molecular chains. Overall, the addition of nano-SiO_2 could have endured with better reinforcement effect of mechanical properties to the obtained nanocomposite films.

3.5. Water contact angle and water vapor permeability

The WCA values of the films without and with nano-SiO_2 were depicted in Fig. 6a. The WCA value of film without nano-SiO_2 was $59.11 \pm 0.62°$, which was lower than those of other four films. The reason might be that molecular interaction formed between nano-SiO_2 and matrix reduced the chance of binding hydrophilic groups to water molecules. Dense spatial structure of nanocomposite films might enhance resistance of the film against liquid water. WCA of film containing 2.5 wt% ($90.41 \pm 3.99°$) nano-SiO_2 was the highest among the WCA values of all kinds of films, and higher than that of SA/cellulose nanocomposite film [41]. The WCA values of nanocomposite films decreased gradually with further increase of the nano-SiO_2 concentration. At low nano-SiO_2 concentration (2.5 and 5 wt%), the hydroxyl groups on the surface of nano-SiO_2 could interact with the hydroxyl groups and carboxylate groups of matrix, which reduced additional active sites for binding of water molecules. Thus, the surplus amount of hydrophilicity residues on the surface of nano-SiO_2 was small. But as nano-SiO_2 concentration further rose, the surplus amount of hydrophilicity residues on the surface of nano-SiO_2 increased gradually, which led to increase in WCA values of nanocomposite film. Overall, the WCA values of films containing 2.5, 5 and 7.5 wt% nano-SiO_2 were all higher than 65 °, indicating that these three films could be regarded as hydrophobic film [3].

The WVP values of AG/SA/SiO_2 nanocomposite film incorporating different concentrations of nano-SiO_2 were illustrated in Fig. 6b. The film without nano-SiO_2 had maximum WVP value among five kinds of films. The WVP of AG/SA was $(8.72 \pm 0.77) \times 10^{-11}$ ($g \cdot m \cdot Pa^{-1} \cdot m^{-2} \cdot s^{-1}$), lower than those of SA/MMT nanocomposite film [24] and AG/lignin/silver nanocomposite film [42]. The addition of nano-SiO_2 enhanced the water vapor

Table 1
Thickness, tensile strength (TS), elongation at break (EB) and moisture content (MC) of AG/SA film and AG/SA/SiO_2 nanocomposite film.

Sample	Thickness (μm)	TS (MPa)	EB (%)	MC (%)
AG/SA	50.2 ± 1.17^{b}	45.18 ± 1.34^{a}	33.04 ± 0.40^{a}	20.23 ± 0.52^{c}
AG/SA - 2.5 wt% SiO_2	45.8 ± 2.50^{a}	56.82 ± 6.99^{b}	37.04 ± 2.37^{a}	18.99 ± 0.65^{b}
AG/SA - 5 wt% SiO_2	46.4 ± 0.30^{a}	62.42 ± 4.48^{bc}	41.96 ± 4.23^{b}	18.67 ± 0.56^{b}
AG/SA - 7.5 wt% SiO_2	47.8 ± 2.94^{ab}	68.32 ± 4.34^{cd}	44.24 ± 2.76^{b}	17.82 ± 0.98^{ab}
AG/SA - 10 wt% SiO_2	48.3 ± 1.17^{ab}	74.68 ± 2.23^{d}	52.99 ± 1.65^{c}	17.17 ± 0.51^{a}

Value (means ± stand deviation). Same letters in the same column are not significant ($p > 0.05$).

Please cite this article as: X. Hou, et al., Effect of SiO2 nanoparticle on the physical and chemical properties of eco-friendly agar/sodium alginate nanocomposite film, (2018), https://doi.org/10.1016/j.ijbiomac.2018.09.109

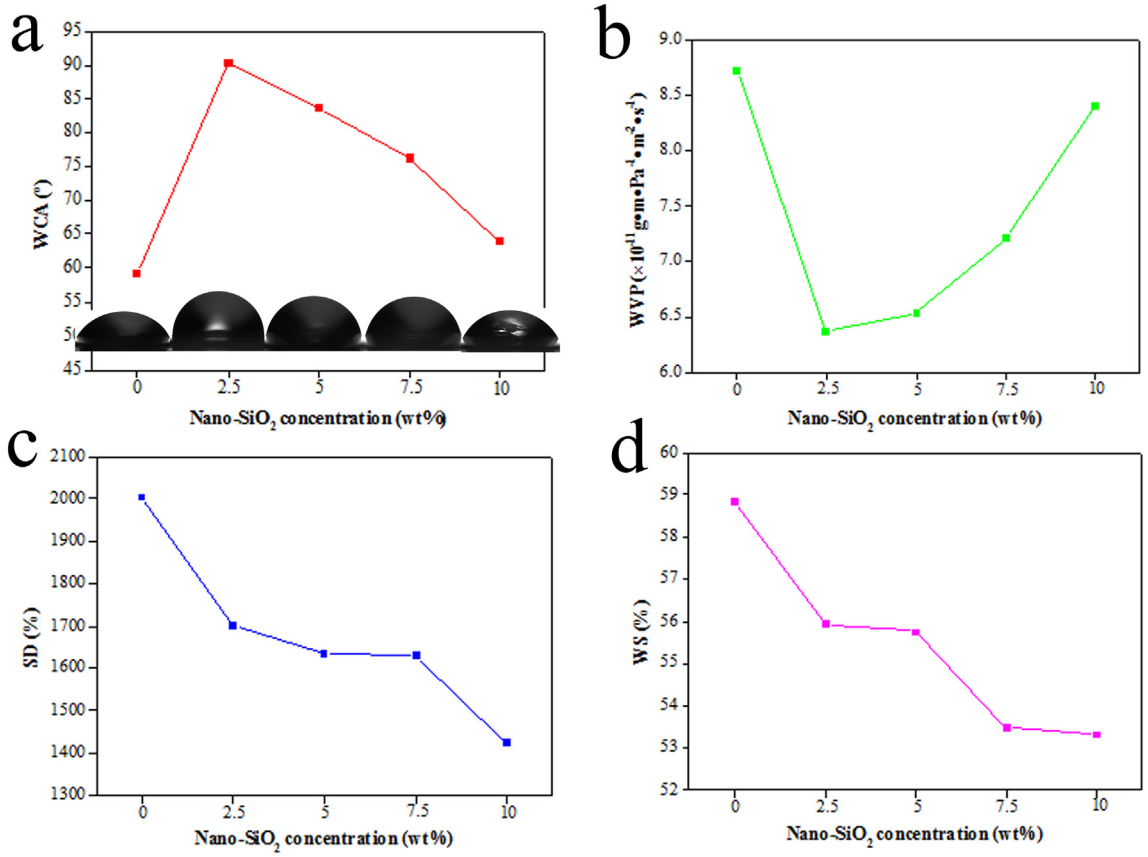

Fig. 6. Trend graph of water contact angle (WCA) (a), water vapor permeability (WVP) (b), swelling degree (SD) (c) and water solubility (WS) (d).

barrier properties of film. The strong interaction formed between nano-SiO_2 and matrix might be conducive to formation of denser polymeric matrix, impeding passing of water molecules through the film [40]. Most nanoparticles with high aspect ratio and good dispersion in the matrix were impermeable. Thus, in order to bypass the SiO_2 nanoparticles, water molecules walked in the film in tortuous path, which extended the path of water molecules through the film. However with increase of nano-SiO_2 concentration, the WVP values of nanocomposite films rose gradually. Although the WCA values of the films containing 2.5, 5 and 7.5 wt% had no significant differences ($p > 0.05$), these values were all significantly lower than that of film without nano-SiO_2 ($p < 0.05$). The diffusion of compounds within edible films and coatings depend strongly on the physicochemical properties of the compounds such as molecular weight, structure, hydrophobicity, and polarity [12]. As nano-SiO_2 concentration rose, the hydrophilicity of nanocomposite film enhanced gradually, evidenced in the result of water contact angle measurement. This enhanced attraction of water molecules to the films, which speeded up the speed of water molecules passing through the film.

3.6. Moisture content, swelling degree and water solubility

The MC values of all the films were shown in the Table 1. The MC value of AG/SA was 20.23 ± 0.52, significantly higher than those of films with nano-SiO_2 ($p < 0.05$). The MC value decreased gradually as the nano-SiO_2 concentration rose, consistent with the result reported by Abdollahi et al. [41]. The phenomenon demonstrated that the addition of nano-SiO_2 decreased the MC of polysaccharide film. This might be ascribed to the interaction formed between nano-SiO_2 and polysaccharide. Hydrogen bonding was formed between the hydroxyl groups on the surface of nano-SiO_2 and hydrophilic groups of matrix, which reduced the contact between water molecules and hydrophilic groups of nanocomposite films. Had been confirmed in mechanical properties, more hydrogen bondings were formed between nano-SiO_2 and matrix at high nano-SiO_2 concentration. Thus, the film with 10 wt% SiO_2 had the lowest MC value among these of five kinds of films.

As one of the most important issues in biodegradable or edible films, water sensitivity implies water resistance during use on the surface of food product and affects the biodegradability of films when applied as packaging materials [43]. SD and WS values of films without and with nano-SiO_2 were depicted in Fig. 6. As can been seen, the SD of film without nano-SiO_2 was 2002 ± 21.95%, significantly higher than those of four other films ($p < 0.05$). This phenomenon demonstrated that the addition of nano-SiO_2 in the film significantly decreased the SD of nanocomposite. This might be attributed to the formation of hydrogen bonding between nano-SiO_2 and matrix. The formed strong interaction decreased average intermolecular distances, which reduced the empty volume of molecular skeleton where water molecules were located. Upon increasing the nano-SiO_2 concentration from 2.5 to 10 wt%, SD value of nanocomposite film decreased gradually up to 1423 ± 17.68, lower than those of AG/carrageenan/clay nanocomposite film and AG/alginate/cellulose/sliver nanocomposite film reported by Rhim et al. [13,37]. The strong interaction enhanced gradually with increasing the nano-SiO_2 concentration, further reducing the empty volume of molecular skeleton. And SiO_2 nanoparticles had already occupied a part of empty volume, which further limited the entry of water molecules into molecular skeleton of matrix.

Similarly to SD trend, WS of film without nano-SiO_2 was 58.84 ± 0.80%, significantly higher than those of film containing nano-SiO_2 ($p < 0.05$). The WS of nanocomposite film decreased gradually as nano-SiO_2 concentration rose, which might also be related to the formation of hydrogen bonding. As for AG/SA film, the chains of molecules were linked only in the form of hydrogen bonding. The

Please cite this article as: X. Hou, et al., Effect of SiO2 nanoparticle on the physical and chemical properties of eco-friendly agar/sodium alginate nanocomposite film, (2018), https://doi.org/10.1016/j.ijbiomac.2018.09.109

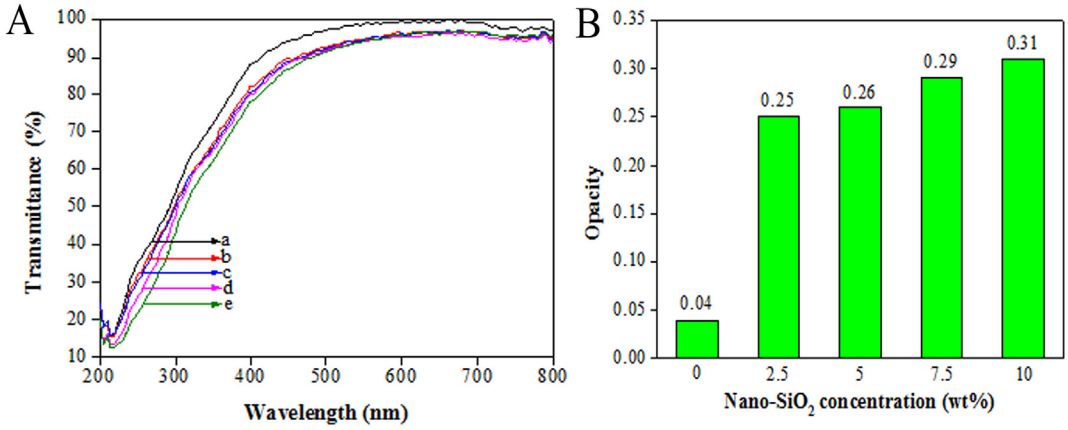

Fig. 7. The diagram of transmittance (A) and opacity (B) of films (a: AG/SA; b: AG/SA - 2.5 wt% SiO_2; c: AG/SA - 5 wt% SiO_2; d: AG/SA - 7.5 wt% SiO_2; e: AG/SA - 10 wt%).

weak interaction between the molecular chains provided the chances for water molecule to contact hydrophilic groups of polysaccharide chains. In three-dimensional spatial structure, the strong interaction formed between nano-SiO_2 and matrix molecule made the link between molecular chains more tight, which restricted the damage of water molecule to the film. The more the interaction forces formed between nano-SiO_2 and matrix were, the stronger the water resistance of nanocomposite film was.

3.7. Optical properties

The result of spectroscopic scanning at wavelengths between 200 and 800 nm of AG/SA film containing different concentration nano-SiO_2 was depicted in Fig. 7. The transmittance of film without nano-SiO_2 was so high that it was close 100% at wavelengths between 500 and 800 nm. As shown in Fig. 7a, in this visible region, the addition of nano-SiO_2 decreased the transmittance of nanocomposite films, but their transmittance was slightly affected by the nano-SiO_2 concentration. The transmittance of AG/cellulose nanocomposite film at 660 nm was below 90% [3]. When the wavelength was <400 nm, the transmittance of all films declined sharply with the decrease of wavelength. In UV region, the transmittance of films decreased gradually as nano-SiO_2 concentration rose, which was attributed to the amount of nano-SiO_2 homogeneously dispersing in the film. This phenomenon indicated that high concentration nano-SiO_2 could be apt to absorb UV belonging to short-wave light than infrared belonging to long-wave light. The reason presumably was related to high aspect ratio and aggregated structure of SiO_2 nanoparticles. The interaction formed between nano-SiO_2 and matrix molecules did not hinder the absorption or reflection of UV and visible light by nano-SiO_2. The ultraviolet and visible light was prone to cause lipid oxidation and food deterioration. Thus, the addition of nano-SiO_2 would have potential application in delaying lipid oxidation of photosensitive foods.

The opacity of films without and with nano-SiO_2 was shown in Fig. 7b. The opacity value of film without nano-SiO_2 was 0.04, significantly lower than those of other four films ($p < 0.05$). The transparency of AG/SA film was obviously higher than those of alginate film and AG film reported by Abdollahi [41] and Rhim [44], respectively. The difference might have been caused by the source of polysaccharide source or experimental condition. With increase of nano-SiO_2 concentration, the opacity rose gradually, indicating that the transparency of nanocomposite film decreased gradually. As shown in SEM, few agglomerated SiO_2 nanoparticles appeared on the surface of film, which might influence the absorption or reflection of visible light by polysaccharide film. And this further demonstrated nano-SiO_2 dispersed homogeneously in the molecular skeleton of polysaccharide. Overall, the addition of nano-SiO_2 enhanced the ultraviolet light resistance of nanocomposite films, but decreased their transparency.

3.8. Film surface color

The edible biodegradable films should be as close to colorless as possible to simulate the appearance of common polymeric films [45]. The L*, a*, b*, ΔE, and WI values of all films were listed in the Table 2. The L* and b* values of films all significantly increased gradually as nano-SiO_2 concentration rose from 0 to 10 wt% ($p < 0.05$), indicating that the addition of nano-SiO_2 increased the luminosity of film and made the film become more yellowish. The a* values of film without nano-SiO_2 significantly lower than those of films containing different concentration nano-SiO_2 ($p < 0.05$). Although the a* values increased gradually with increase of nano-SiO_2 concentration, there were slight differences between their a* values ($p > 0.05$). However, Vejdan et al. reported that the concentration of nano-TiO_2 significantly influenced the a* values of AG/gelation/TiO_2 nanocomposite film [38]. This phenomenon demonstrated that the color of film became reddish when nano-SiO_2 was added into the films, but the concentration of nano-SiO_2 had nonsignificant influence on them. Also, ΔE and WI all enlarged gradually upon increasing nano-SiO_2 concentration. The white color of SiO_2 nanoparticle itself improved the WI of film. However, the WI of film without nano-SiO_2 was higher than those of films containing nano-SiO_2. This reason might be related to the transparency of film and whiteness of white plate. Having been confirmed in the optical properties, the film without

Table 2
Color parameters of AG/SA film and AG/SA/SiO_2 nanocomposite film.

Sample	L*	a*	b*	ΔE	WI
AG/SA	88.32 ± 0.09^{a}	7.45 ± 0.08^{a}	7.55 ± 0.02^{a}	4.49 ± 0.09^{a}	84.46 ± 0.12^{c}
AG/SA - 2.5 wt% SiO_2	88.77 ± 0.01^{b}	7.89 ± 0.01^{b}	8.20 ± 0.07^{b}	4.57 ± 0.04^{ab}	83.48 ± 0.21^{a}
AG/SA - 5 wt% SiO_2	88.91 ± 0.04^{c}	7.94 ± 0.23^{b}	8.34 ± 0.03^{c}	4.58 ± 0.02^{ab}	84.01 ± 0.43^{b}
AG/SA - 7.5 wt% SiO_2	89.25 ± 0.02^{d}	8.02 ± 0.31^{b}	8.66 ± 0.05^{d}	4.62 ± 0.05^{b}	84.17 ± 0.10^{bc}
AG/SA - 10 wt% SiO_2	89.47 ± 0.08^{e}	8.16 ± 0.16^{b}	8.97 ± 0.01^{e}	4.76 ± 0.04^{c}	84.21 ± 0.13^{bc}

Value (means ± stand deviation). Same letters in the same column are not significant ($p > 0.05$).

Please cite this article as: X. Hou, et al., Effect of SiO2 nanoparticle on the physical and chemical properties of eco-friendly agar/sodium alginate nanocomposite film, (2018), https://doi.org/10.1016/j.ijbiomac.2018.09.109

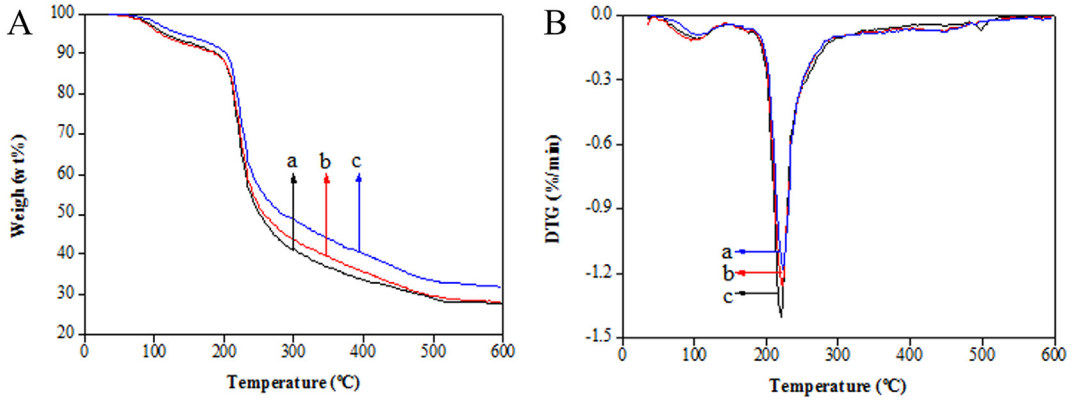

Fig. 8. TG (A) and DTG (B) thermograms of films (a: AG/SA; b: AG/SA - 5 wt% SiO_2; c: AG/SA - 10 wt% SiO_2).

nano-SiO_2 had the highest transparency among those of five kinds of films. Thus, WI of film was easily influenced by white color of white plate.

3.9. Thermal stability

The thermal stability of films containing 0, 5, 10 wt% nano-SiO_2 was examined by thermogravimetric analysis. The TG and differential TG (DTG) curves were presented in Fig. 8 and the data of thermal stability was shown in Table 3. The first step of weight loss occurred at 50–150 °C, corresponding to the loss of absorbed and bound water. The second stage of weight loss was 160–310 °C, due to the thermal destruction of the glycosidic bond and the elimination of adjacent hydroxyl group, which resulted in the formation of the intermediate material [27]. The third step, for temperature higher than 310 °C, attributed to the residual decomposition reaction and char formation [46]. Initially, the decomposition onset temperature (T_{onset}) of AG/SA film was 115 °C, higher than that of film containing 5 wt% nano-SiO_2, but lower than that of film containing 10 wt% nano-SiO_2. At the 5 wt% nano-SiO_2 concentration, the addition of nano-SiO_2 accelerated the film dehydration. However, the addition of high concentration nano-SiO_2 in film delayed the film dehydration, which might be attributed the evaporation of water from nano-SiO_2. The temperature corresponding to the maximum degradation rate (T_{max}) and char production at 600 °C both increased gradually as the nano-SiO_2 concentration rose, indicating that the addition of nano-SiO_2 enhanced the thermal stability of nanocomposite film. The reason might be related to the interaction formed between nano-SiO_2 and matrix. High temperature resistance of nano-SiO_2 also might have the favorable effect on improving the thermal stability of nanocomposite film.

4. Conclusion

AG/SA nanocomposite films were prepared through solution casting method incorporating different nano-SiO_2 concentration. The mechanical properties, water resistance, optical properties, and color of film surface of five kinds of film were tested. SEM and XRD showed that nano-SiO_2 dispersed homogeneously in the films. FTIR demonstrated that hydrogen bonding was formed between nano-SiO_2 and molecules of matrix. The TS and EB of film containing 10 wt% nano-SiO_2 increased by 65.29% and 60.38% respectively when compared to those of film prepared without nano-SiO_2. The addition of nano-SiO_2 significantly enhanced the mechanical properties of nanocomposite films, which might be ascribed to the formation of interaction forces. As the filler, nanoscale SiO_2 particles improved the property of mutual rearrangements of chain unit. The film containing 2.5 wt% nano-SiO_2 had maximum water contact angle and minimum water vapor permeability among these of five kinds of films, indicating that low concentration nano-SiO_2 could enhance hydrophobicity of film. However, the film containing 10 wt% nano-SiO_2 had minimum swelling degree and water solubility when compared to those of other films, further demonstrating the formation of strong interaction. This result demonstrated that the addition of nano-SiO_2 improved the stability of the films in water. Nano-SiO_2 enhanced the properties of film against UV light, while it decreased their transparency. The film containing 10 wt% nano-SiO_2 had best thermal stability. Overall, the addition of nano-SiO_2 enhanced the mechanical properties, water resistance, barrier properties against UV light, and thermal stability of film. Thus, the results suggested that the AG/SA nanocomposite films containing appropriate concentration nano-SiO_2 can be used as food packaging materials. However, further studies are still required to apply on real food systems.

Table 3
The data of thermal stability of AG/SA film and AG/SA/SiO_2 nanocomposite film.

Sample	T_{onset} (°C)	T_{max} (°C)	Char 600 °C (wt%)
AG/SA	115	220	27.89
AG/SA - 5 wt% SiO_2	110	222	28.18
AG/SA - 10 wt% SiO_2	137	223	31.73

Acknowledgements

This work was supported by the National High Technology Research and Development Program of China (2010AA093701), the National Natural Science Foundation of China (Grant 50803030), the Program for Changjiang Scholars and Innovative Research Team in University (IRT0970), the Postdoctoral Science Special Foundation of China (201104581), the Postdoctoral Science Foundation of China (20100471495), the Program for Excellent Innovative Research Team of Shandong Province, China (TD200902).

References

[1] M. Abdollahi, M. Alboofetileh, M. Rezaei, R. Behrooz, Comparing physico-mechanical and thermal properties of alginate nanocomposite films reinforced with organic and/or inorganic nanofillers, Food Hydrocoll. 32 (2013) 416–424.
[2] T. Garrido, A. Etxabide, P. Guerrero, K. de la Caba, Characterization of agar/soy protein biocomposite films: effect of agar on the extruded pellets and compression moulded films, Carbohydr. Polym. 151 (2016) 408–416.
[3] S. Shankar, J.W. Rhim, Preparation of nanocellulose from micro-crystalline cellulose: the effect on the performance and properties of agar-based composite films, Carbohydr. Polym. 135 (2016) 18–26.
[4] Y.A. Arfat, J. Ahmed, H. Jacob, Preparation and characterization of agar-based nanocomposite films reinforced with bimetallic (Ag-Cu) alloy nanoparticles, Carbohydr. Polym. 155 (2017) 382–390.
[5] V.D. Alves, N. Costa, I.M. Coelhoso, Barrier properties of biodegradable composite films based on kappa-carrageenan/pectin blends and mica flakes, Carbohydr. Polym. 79 (2010) 269–276.
[6] X. Zhao, Q. Li, X. Ma, F. Quan, J. Wang, Y. Xia, The preparation of alginate–AgNPs composite fiber with green approach and its antibacterial activity, J. Ind. Eng. Chem. 24 (2015) 188–195.

Please cite this article as: X. Hou, et al., Effect of SiO2 nanoparticle on the physical and chemical properties of eco-friendly agar/sodium alginate nanocomposite film, (2018), https://doi.org/10.1016/j.ijbiomac.2018.09.109

[7] S. Mohajer, M. Rezaei, S.F. Hosseini, Physico-chemical and microstructural properties of fish gelatin/agar bio-based blend films, Carbohydr. Polym. 157 (2017) 784–793.

[8] J.W. Rhim, L.F. Wang, Mechanical and water barrier properties of agar/κ-carrageenan/konjac glucomannan ternary blend biohydrogel films, Carbohydr. Polym. 96 (2013) 71–81.

[9] V. Paşcalău, V. Popescu, G.L. Popescu, M.C. Dudescu, G. Borodi, A. Dinescu, I. Perhaiţa, M. Paul, The alginate/k-carrageenan ratio's influence on the properties of the cross-linked composite films, J. Alloys Compd. 536 (2012) S418–S423.

[10] K.C. Labropoulos, D.E. Niesz, S.C. Dabforth, P.G. Kevreekidis, Dynamic rheology of agar gels: theory and experiment. Part I. Development of a rheological model, Carbohydr. Polym. 50 (2002) 393–406.

[11] J.W. Rhim, Effect of clay contents on mechanical and water vapor barrier properties of agar-based nanocomposite films, Carbohydr. Polym. 86 (2011) 691–699.

[12] E. Tavassoli-Kafrani, H. Shekarchizadeh, M. Masoudpour-Behabadi, Development of edible films and coatings from alginates and carrageenans, Carbohydr. Polym. 137 (2016) 360–374.

[13] J.W. Rhim, Effect of PLA lamination on performance characteristics of agar/κ-carrageenan/clay bio-nanocomposite film, Food Res. Int. 51 (2013) 714–722.

[14] M. Atef, M. Rezaei, R. Behrooz, Preparation and characterization agar-based nanocomposite film reinforced by nanocrystalline cellulose, Int. J. Biol. Macromol. 70 (2014) 537–544.

[15] L.F. Wang, S. Shankar, J.W. Rhim, Properties of alginate-based films reinforced with cellulose fibers and cellulose nanowhiskers isolated from mulberry pulp, Food Hydrocoll. 63 (2017) 201–208.

[16] J.J. Zhou, S.Y. Wang, S. Gunasekaran, Preparation and characterization of whey protein film incorporated with TiO2 nanoparticles, J. Food Sci. 74 (2009) N50–N56.

[17] P. Fabbri, B. Singh, Y. Leterrier, J.A.E. Manson, M. Messori, F. Pilati, Cohesive and adhesive properties of polycaprolactone/silica hybrid coatings on poly(methyl methacrylate) substrates, Surf. Coat. Technol. 200 (2006) 6706–6712.

[18] N. Garia, T. Corrales, J. Guzman, P. Tiemblo, Understanding the role of nanosilica particle surfaces in the thermal degradation of nano silica-poly(methyl methacrylate) solution-blended nanocomposites: from low to high silica concentration, Polym. Degrad. Stab. 92 (2007) 635–643.

[19] K.C. Kavya, R. Jayakumar, S. Nair, K.P. Chennazhi, Fabrication and characterization of chitosan/gelatin/nSiO2 composite scaffold for bone tissue engineering, Int. J. Biol. Macromol. 59 (2013) 255–263.

[20] M. Mehrasa, M.A. Asadollahi, K. Ghaedi, H. Salehi, A. Arpanaei, Electrospun aligned PLGA and PLGA/gelatin nanofibers embedded with silica nanoparticles for tissue engineering, Int. J. Biol. Macromol. 79 (2015) 687–695.

[21] M. Hassannia-Kolaee, F. Khodaiyan, R. Pourahmad, I. Shahabi-Ghahfarrokhi, Development of ecofriendly bionanocomposite: whey protein isolate/pullulan films with nano-SiO_2, Int. J. Biol. Macromol. 86 (2016) 139–144.

[22] J.W. Rhim, S.B. Lee, S.I. Hong, Preparation and characterization of agar/clay nanocomposite films: the effect of clay type, J. Food Sci. 76 (2011) N40–N48.

[23] Y. Pranoto, S.K. Rakshit, V.M. Salokhe, Enhancing antimicrobial activity of chitosan films by incorporating garlic oil, potassium sorbate and nisin, LWT Food Sci. Technol. 38 (2005) 859–865.

[24] M. Alboofetileh, M. Rezaei, H. Hosseini, M. Abdollahi, Effect of montmorillonite clay and biopolymer concentration on the physical and mechanical properties of alginate nanocomposite films, J. Food Eng. 117 (2013) 26–33.

[25] J.B. Xu, J.P. Bartley, R.A. Johnson, Preparation and characterization of alginate–carrageenan hydrogel films crosslinked using a water-soluble carbodiimide (WSC), J. Membr. Sci. 218 (2003) 131–146.

[26] S. Tunc, H. Angellier, Y. Cahyana, P. Chalier, N. Gontard, E. Gastaldi, Functional properties of wheat gluten/montmorillonite nanocomposite films processed by casting, J. Membr. Sci. 289 (2007) 159–168.

[27] M. Yang, Y. Xia, Y. Wang, X. Zhao, Z. Xue, F. Quan, C. Geng, Z. Zhao, Preparation and property investigation of crosslinked alginate/silicon dioxide nanocomposite films, J. Appl. Polym. Sci. 133 (2016) 43489.

[28] M. Yang, J. Shi, Y. Xia, Effect of SiO_2, PVA and glycerol concentrations on chemical and mechanical properties of alginate-based films, Int. J. Biol. Macromol. 107 ((2018) 2686–2694.

[29] Q. Cao, Y. Zhang, W. Chen, X. Meng, B. Liu, Hydrophobicity and physicochemical properties of agarose film as affected by chitosan addition, Int. J. Biol. Macromol. 106 (2018) 1307–1313.

[30] S. Tang, P. Zou, H. Xiong, H. Tang, Effect of nano-SiO_2 on the performance of starch/polyvinyl alcohol blend films, Carbohydr. Polym. 72 (2008) 521–526.

[31] P. Sambyal, G. Ruhi, S.K. Dhawan, B.M.S. Bisht, S.P. Gairola, Enhanced anticorrosive properties of tailored poly(aniline-anisidine)/chitosan/SiO_2 composite for protection of mild steel in aggressive marine conditions, Prog. Org. Coat. 119 (2018) 203–213.

[32] S. Iftekhar, V. Srivastava, A. Casas, M. Sillanpää, Synthesis of novel GA-g-PAM/SiO_2 nanocomposite for the recovery of rare earth elements (REE) ions from aqueous solution, J. Clean. Prod. 170 (2018) 251–259.

[33] A. Watthanaphanit, P. Supaphol, H. Tamura, S. Tokura, R. Rujiravanit, Wet-spun alginate/chitosan whiskers nanocomposite fibers: preparation, characterization and release characteristic of the whiskers, Carbohydr. Polym. 79 (2010) 738–746.

[34] E. Gómez-Ordóñez, P. Rupérez, FTIR-ATR spectroscopy as a tool for polysaccharide identification in edible brown and red seaweeds, Food Hydrocoll. 25 (2011) 1514–1520.

[35] L. Pereira, A. Sousa, H. Coelho, A.M. Amado, P.J.A. Ribeiro-Claro, Use of FTIR, FT-Raman and 13C-NMR spectroscopy for identification of some seaweed phycocolloids, Biomol. Eng. 20 (2003) 223–228.

[36] S. Shankar, L.F. Wang, J.W. Rhim, Preparations and characterization of alginate/silver composite films: effect of types of silver particles, Carbohydr. Polym. 146 (2016) 208–216.

[37] L.F. Wang, J.W. Rhim, Preparation and application of agar/alginate/collagen ternary blend functional food packaging films, Int. J. Biol. Macromol. 80 (2015) 460–468.

[38] A. Vejdan, S.M. Ojagh, A. Adeli, M. Abdollahi, Effect of TiO_2 nanoparticles on the physico-mechanical and ultraviolet light barrier properties of fish gelatin/agar bilayer film, LWT Food Sci. Technol. 71 (2016) 88–95.

[39] H.C. Voon, R. Bhat, A.M. Easa, M.T. Liong, A.A. Karim, Effect of addition of halloysite nanoclay and SiO_2 nanoparticles on barrier and mechanical properties of bovine gelatin films, Food Bioprocess Technol. 5 (2012) 1766–1774.

[40] R.H. Tabatabaei, S.M. Jafari, H. Mirzaei, A.M. Nafchi, D. Dehnad, Preparation and characterization of nano-SiO_2 reinforced gelatin-k-carrageenan biocomposites, Int. J. Biol. Macromol. 111 (2012) 1091–1099.

[41] M. Abdollahi, M. Alboofetileh, R. Behrooz, M. Rezaei, R. Miraki, Reducing water sensitivity of alginate bio-nanocomposite film using cellulose nanoparticles, Int. J. Biol. Macromol. 54 (2013) 166–173.

[42] S. Shankar, J.W. Rhim, Preparation and characterization of agar/lignin/silver nanoparticles composite films with ultraviolet light barrier and antibacterial properties, Food Hydrocoll. 71 (2017) 76–84.

[43] M.A. Cerqueira, B.W.S. Souza, J.A. Teixeira, A.A. Vicente, Effect of glycerol and corn oil on physicochemical properties of polysaccharide films – a comparative study, Food Hydrocoll. 27 (2012) 175–184.

[44] J.W. Rhim, Physical-mechanical properties of agar/κ-carrageenan blend film and derived clay nanocomposite film, J. Food Sci. 77 (2012) N66–N73.

[45] J.W. Rhim, A. Gennadios, C.L. Weller, M.A. Hanna, Sodium dodecyl sulfate treatment improves properties of cast films from soy protein isolate, Ind. Crop. Prod. 15 (2002) 199–205.

[46] K.M.A. Uddin, M. Ago, O.J. Rojas, Hybrid films of chitosan, cellulose nanofibrils and boric acid: flame retardancy, optical and thermo-mechanical properties, Carbohydr. Polym. 177 (2017) 13–21.

Please cite this article as: X. Hou, et al., Effect of SiO2 nanoparticle on the physical and chemical properties of eco-friendly agar/sodium alginate nanocomposite film, (2018), https://doi.org/10.1016/j.ijbiomac.2018.09.109